

Interference of nematic quantum critical quasiparticles: a route to the octet model

Eun-Ah Kim¹ and Michael J. Lawler^{2,1}

¹*Department of Physics, Cornell University, Ithaca, NY 14853*

²*Department of Physics, Binghamton University, Binghamton NY 13902*

(Dated: November 6, 2018)

Repeated observations of inhomogeneity in cuprate superconductors[1, 2, 3, 4, 5] make one immediately question the existence of coherent quasiparticles(qp's) and the applicability of a momentum space picture. Yet, observations of interference effects[6, 7, 8, 9] suggest that the qp's maintain a remarkable coherence under special circumstances. In particular, quasi-particle interference (QPI) imaging using scanning tunneling spectroscopy revealed a highly unusual form of coherence: accumulation of coherence only at special points in momentum space with a particular energy dispersion[5, 6, 7]. Here we show that nematic quantum critical fluctuations[10], combined with the known extreme velocity anisotropy[11] provide a natural mechanism for the accumulation of coherence at those special points. Our results raise the intriguing question of whether the nematic fluctuations provide the unique mechanism for such a phenomenon.

The capability of QPI studies in inferring momentum space electronic structure from real space local density of states(LDOS) images is surprising given the strong presence of glassiness and nanoscale inhomogeneity in cuprate superconductors. The simplicity of the QPI image, a set of well defined dispersing peaks, is particularly striking considering the complexity of the real space image. McElroy et al. [6] made an insightful observation: the peak positions are determined by the eight tips of the “banana” shaped qp equal energy contours. However, a key question remains of this “octet model” — what makes the qp's at the tips especially coherent to the extent that only interference among qp's at the tips remain visible.

Underlying the QPI interpretation of the Fourier transform of the LDOS map $N(\vec{r}, \omega)$, is the assumption that the modulated contribution $\tilde{N}_{imp}(\vec{q}, \omega)$ results from coherent qp's scattering off sparsely distributed impurities. For conventional metals where these assumptions hold, the modulations in LDOS can be understood in terms of interference among single particle wave functions[12]. Naturally, there has been much effort towards interpreting the QPI in cuprates also in terms of free (Bogoliubov) qp pictures [13, 14, 15]. Surprisingly, these free QPI patterns are far more intricate than the set of simple dispersing peaks observed in the experiment. Hence one might view this as a rare circumstance in which an experimental message is much simpler than that provided by the simplest theory.

What is necessary to explain QPI in the cuprates, given these free theory results, is to introduce scattering among the electrons in such a way that only the banana tip qp's remain coherent. Recently, together with our collaborators, we have shown[10] that such a phenomenon naturally occurs at the nodal nematic quantum critical point (QCP) of a d-wave superconductor. “Nematic” here refers to a broken symmetry phase in which the fourfold rotational symmetry of the crystal is broken down to a twofold symmetry (see Fig. 1(a)). In a d-wave super-

conductor, such additional symmetry breaking results in a shifting of the nodal positions away from their fourfold symmetric locations[16]. At the nodal nematic QCP, we found[10] that the softening of the nodal positions introduces strongly \vec{k} dependent decoherence that brings in stark contrast between the tips of the banana, where qp's remain coherent with long lifetime, and the rest of the equal energy contour, where qp's get severely damped (see Fig. 1(b) and (c)).

Here we show that \vec{k} dependent decoherence due to nematic fluctuations leads to the very simplification observed in QPI experiments: peaks in fourier transform LDOS. We further argue for the uniqueness of this route based on the severely restricted qp scattering mechanisms in a d-wave superconductor due to their limited phase space[16] combined with the following experimental evidence supporting the existence of nematic ordering in underdoped cuprates. Hinkov et al. [17] found direct evidence for nematic ordering in $\text{YBa}_2\text{Cu}_3\text{O}_{6.45}$. Furthermore, both the glassy nematic behavior in underdoped $\text{Bi}_2\text{Sr}_2\text{CaCu}_2\text{O}_{8+\delta}$ [5] and the doping dependent flattening of the near-node gap slope $\text{Bi}_2\text{Sr}_2\text{CaCu}_2\text{O}_{8+\delta}$ [7, 18, 19] can be naturally explained by an increasing degree of nematicity upon underdoping.

In a many-body setting, a crisp way to capture the modulation of LDOS resulting from isolated impurities is to use the T-matrix formalism (see for example Ref. [15]) which expresses the energy resolved LDOS $\tilde{N}_{imp}(\vec{q}, \omega)$ at wave vector \vec{q} as

$$\tilde{N}_{imp}(\vec{q}, \omega) = -2\text{sgn}(\omega)\text{Im} \int d\vec{k} \left[\hat{\mathcal{G}}(\vec{k} + \vec{q}, \omega) \hat{T} \hat{\mathcal{G}}(\vec{k}, \omega) \right]_{11} \quad (1)$$

where $\hat{\mathcal{G}}(\vec{k}, \omega)$ is the (2×2) single particle Nambu matrix propagator in a superconducting state without impurity scattering and \hat{T} is the impurity potential in the weak (perturbative) impurity limit. Here \hat{T} depends on the type of impurity. For a charge impurity which is anti-symmetric in Nambu space, $\hat{T} = V_c \hat{\sigma}_3$, while $\hat{T} = V_m \mathbb{I}$

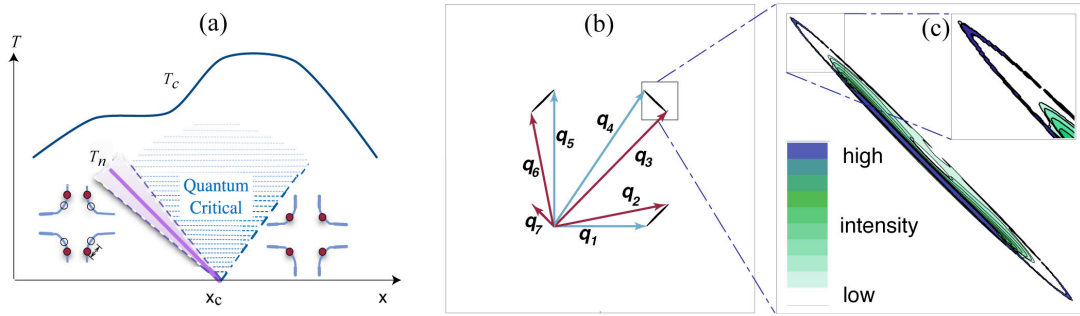


FIG. 1: The electron spectral distribution at the nodal nematic quantum critical point in the linearized approximation (taken from Ref. [10]). (a) proposed phase diagram inside the superconducting dome, where x is a tuning parameter. Note the change in location of the nodes through the phase transition. (b) Equal energy contour at $\omega = 3\text{meV}$ and the connecting \vec{q} -vectors of the banana tips. The \vec{q}_i are colored blue and red depending on whether they connect \vec{k} points with the same or opposite sign of the d -wave gap $\Delta_{\vec{k}}$. (c) blowup of the momentum distribution $A(\vec{k}, \omega = 3\text{meV})$ of the spectral function near one node. Note the sharpness of the momentum distribution at the banana tip shown in the inset.

for a magnetic impurity and $\hat{T} = V_{\Delta}\hat{\sigma}_1$ for a superconducting gap impurity, both of which are symmetric in Nambu space ($\hat{\sigma}_i$ are Pauli matrices acting on Nambu spinor).

Equation(1) shows that $\tilde{N}_{imp}(\vec{q}, \omega)$ is the amplitude modulation associated with the overlap between two qp states with wave vector \vec{k} and $\vec{k} + \vec{q}$ scattering off the impurity. Hence $\tilde{N}_{imp}(\vec{q}, \omega)$ will show high intensity at a special vector \vec{q} , if it connects two coherent (long lived) qp states with the same energy ω constructively. McElroy et al. [6] and Wang and Lee [13] noticed that the density of state $Im\hat{G}$ is accumulated at the \vec{k} points at the eight tips of the “banana” contours. In fact, a comparison between auto-correlation analysis of ARPES spectra and the QPI study of the same system showed remarkable similarity demonstrating this principle[21]. However, this similarity is not reproduced by calculations of relevant quantities. Hence peaks observed in QPI requires a mechanism that goes beyond accumulation of states and makes the tips especially coherent. Such mechanism has been a theoretical mystery.

The nature of the propagating single qp states is encoded in the Nambu matrix propagator \hat{G} entering equation(1). If, in between impurity scattering events, the qp’s experience collisions with critical nematic collective modes, a self energy $\hat{\Sigma}$ is induced (see e.g., Ref. [22])

$$\hat{G}^{-1} = \hat{G}_0^{-1} - \hat{\Sigma}. \quad (2)$$

Here \hat{G}_0 is the free Bogoliubov qp propagator of a BCS superconductor. In order to capture the nematic critical fluctuations, we use the self-energy obtained in Ref.[10].

In the context of the cuprates, $\hat{G}_0(\vec{k}, \omega)$ takes the form

$$\hat{G}_0^{-1} = (\omega + i\delta)\mathbb{I} - \varepsilon_{\vec{k}}\sigma_3 - \Delta_{\vec{k}}\sigma_1 \quad (3)$$

where $\varepsilon_{\vec{k}}$ is the dispersion of normal state qp’s and $\Delta_{\vec{k}} = \Delta_0(\cos k_x a - \cos k_y a)$ is the d -wave pairing amplitude. In the low energy long wavelength limit, we can approximate this \hat{G}_0 by linearizing around the four gapless

nodal points $\vec{k} \approx \vec{K}$ where the qp energy $\xi_{\vec{k}} = \sqrt{\varepsilon_{\vec{k}}^2 + \Delta_{\vec{k}}^2}$ vanishes:

$$\mathcal{G}_0^{-1} \Big|_{\text{near node } \vec{K}} = (\omega + i\delta)\mathbb{I} - v_F(k_x - K_x)\hat{\sigma}_3 - v_{\Delta}(k_y - K_y)\hat{\sigma}_1. \quad (4)$$

Linearizing $\varepsilon_{\vec{k}}$ and $\Delta_{\vec{k}}$ given in Ref.[23] based on photoemission data, we find $v_F = 0.508$ and $v_{\Delta} = 0.025$ in units of $eV(a/\pi)$. (Note that the resulting anisotropy ratio $v_F/v_{\Delta} = 20.3$ is large and consistent with the value of 19 inferred from thermal conductivity measurements[11].)

The effect of nematic critical fluctuations in the QPI intensity is evident when compared with free linearized Bogoliubov qp’s. In Fig.2(a), we plot the QPI intensity $\tilde{N}_{imp}(\vec{q}, \omega = 9\text{meV})$ for the free qp’s with $\hat{G} = \hat{G}_0$ induced by charge impurities $\hat{T} = V_C\hat{\sigma}_3$. Most noticeable features in Fig.2 (a) are the extended and broad line shaped segments and the less extended but faint patterns. The vectors \vec{q}_i connecting the tips of bananas shown in Fig. 1(b) are overlaid on the intensity plot in Fig.2(b) and (c). Clearly, \vec{q}_3, \vec{q}_4 and \vec{q}_7 land on the broad line shaped segments but the rest of \vec{q}_i vectors point to very faint features. This is inconsistent with the experiments showing well defined peaks at all \vec{q}_i vectors albeit with varying intensities.

The most dramatic change that nematic quantum critical fluctuations introduces in the QPI intensity, is the octet peak structure. Comparing the QPI intensity plot of Fig. 2(b) for nematic quantum critical qp’s in the presence of charge impurities to that of Fig. 2(a) for free Bogoliubov qp’s, nematic quantum critical qp’s allow for unambiguous identification of all \vec{q}_i vectors. (Note that the intensity is higher for sign reversing scattering vectors $\vec{q}_2, \vec{q}_3, \vec{q}_6$, and \vec{q}_7 when the QPI is due to charge impurities. This is consistent with the trend observed in superconducting $\text{Bi}_2\text{Sr}_2\text{CaCu}_2\text{O}_{8+\delta}$ [5, 6, 7, 20].) Such contrast between free qp’s and nematic quantum critical qp’s are more quantitatively displayed in line cuts in

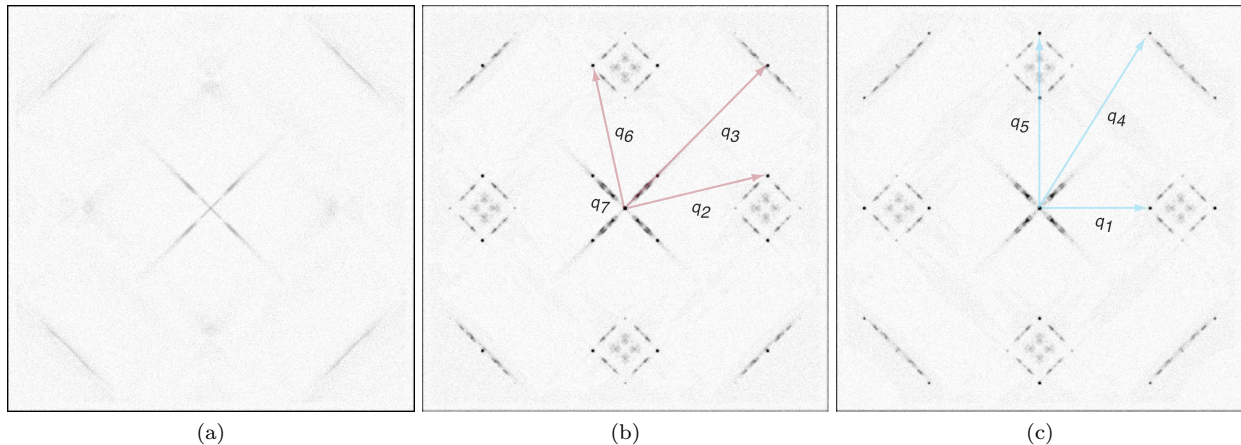


FIG. 2: (a) QPI Fourier amplitudes $|N(q_x, q_y, \omega = 9\text{meV})|$ for free Bogoliubov qp's with linearized dispersion. (b) QPI Fourier amplitudes at the nematic QCP in the presence of scalar (non-magnetic) impurities (\vec{q}_i , $i = \{2, 3, 6, 7\}$ label the constructively interfering peaks) (c) QPI Fourier amplitudes at the nematic QCP in the presence of magnetic impurities (\vec{q}_i , $i = \{1, 4, 5\}$ label the constructively interfering peaks). The \vec{q}_i vectors, defined in Fig. 1(b) are precisely those specified in the octet model of Ref. 6 . Note that at all \vec{q}_i the QPI Fourier amplitudes are dramatically enhanced at the Nematic QCP. We used a gray scale where black represents intensities greater than a fixed threshold that is the same for all plots.

Fig.3 along \vec{q}_1 direction and \vec{q}_7 direction.

The fact that nematic critical fluctuations sharpen the interference pattern and reveal positions of \vec{q}_i vectors is rather striking. One generally expects critical fluctuations to blur the already soft features in the interference pattern of the free Bogoliubov qp's in Fig. 2 (a). However, the effect of the critical nematic collective mode is quite the opposite[10]: it sharpens the interference pattern. The nematic critical mode renormalizes the dispersion of the qp's at the tips down, reducing the gap slope v_Δ and enhancing the velocity anisotropy[10, 24] (Intriguingly, systematic flattening of the gap slope with underdoping recently observed in $\text{Bi}_2\text{Sr}_2\text{CaCu}_2\text{O}_{8+\delta}$ [7, 18, 19] could therefore be related to glassy nematicity). This downward renormalization of v_Δ frees the qp's at the tips from further collisions with the nematic mode[10]. However, qp's on the rest of the equal energy contour lose coherence after a finite time τ_k set by $\text{Im}\hat{\Sigma}(\vec{k}, \omega)$ that is inversely proportional to their energy ω .

An unambiguous sign of interference origin of peaks displayed in Fig.2(b) would be to look for signs of constructive and destructive interference. Such distinctions can be found by noting that there are two classes of scattering \vec{q}_i vectors connecting \vec{k} space points in a d -wave superconductor, depending on whether they connect points with the opposite sign of the gap (red in Fig.1 and Fig.2) or the same sign of the gap (blue in the same figures). Each of these classes of \vec{q}_i vectors can be associated with constructive or destructive interference depending on the nature of the impurity scattering center, as it has been pointed out in Refs. [13, 14]. Specifically, since the charged impurity potential is asymmetric

in Nambu space (charged impurities affect particles and holes differently), *sign reversing* \vec{q}_i 's are expected to yield constructive interference. On the other hand, both magnetic impurities $V_m\mathbb{1}$ and pair scattering centers $V_\Delta\hat{\sigma}_1$ which are symmetric in Nambu space are expected to yield constructive interference for *sign preserving* \vec{q}_i 's. What is new here is that nematic critical fluctuations clearly reveal the octet peaks through the accumulation of coherence at the tips in the \vec{k} space equal energy contour, and hence enable sharp comparison between QPI's induced by different types of impurity scattering centers. This reasoning is clearly borne out in the line cuts Fig.3.

One way of tuning the degree of such constructive and destructive interference is to introduce vortices. A vortex can act both as a pair field impurity due to its core and as a magnetic impurity due to screening currents. Since both the pair field impurity and magnetic impurity are symmetric in Nambu space, vortices would shift the QPI intensity towards sign-preserving vectors as shown in Fig. 2(c) and Fig. 3(c). This trend is in remarkable agreement with recent magnetic field dependence studies of QPI[25]. Scattering due to thermally excited vortices should also lead to a similar trend of enhancing peaks at \vec{q}_1 , \vec{q}_4 and \vec{q}_5 upon raising temperature.

In summary, we have shown that nematic critical fluctuations provide a natural mechanism for the accumulation of coherence that can lead to well defined peaks in the QPI map in a manner that is consistent with the existing experimental literature. This is the first case in which the octet vectors \vec{q}_i were unmistakably revealed through a straightforward calculation. One open question is how to resolve the disappearance of the dispersing QPI peaks that accompanies the emergence of nematic

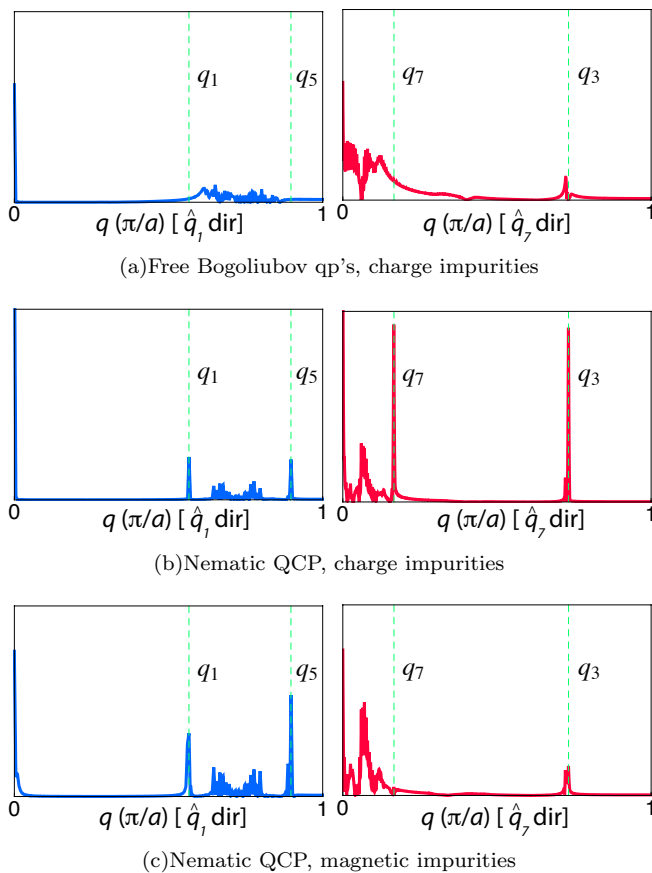


FIG. 3: Normalized LDOS line cuts of the interference signal along the \vec{q}_1 (or [100]) direction and along the \vec{q}_7 (or [110]) direction. All plots have the same y-axis scale. (a) weak features of a BCS d-wave superconductor. At the nematic QCP (b) shows scalar impurities inducing constructive interference at \vec{q}_1 and \vec{q}_5 , and destructive interference at \vec{q}_3 and \vec{q}_7 while (c) shows the opposite behavior for the case of magnetic impurities. QPI due to a pairing impurity $V_{\Delta}\hat{\sigma}_1$ has a qualitatively similar pattern to (c) (not presented).

glass features at high energy scales[7, 20]. This is a subject of future study. However, at this point, perhaps the most tantalizing question one could ask would be whether nematic quantum critical fluctuations provide the unique mechanism for the existence of dispersing QPI peaks.

Acknowledgements We thank J.C. Davis, E. Fradkin, J.E. Hoffman, S. Kivelson, S. Sachdev, J. Sethna, K. Shen, O. Vafek for useful discussions. We thank T. Hanaguri for discussions and sharing his unpublished data.

- 11006–+ (2000).
- [2] C. Howald, R. Fournier, and A. Kapitulnik, Phys. Rev. B **64**10 (2001).
- [3] K. Lang, V. Madhavan, J. Hoffman, E. Hudson, H. Eisaki, S. Uchida, and J. Davis, Nature **415**, 412 (2002).
- [4] M. Vershinin, S. Misra, S. Ono, Y. Abe, Y. Ando, and A. Yazdani, Science **303**, 1995 (2004).
- [5] Y. Kohsaka, C. Taylor, K. Fujita, A. Schmidt, C. Lupien, T. Hanaguri, M. Azuma, M. Takano, H. Eisaki, H. Takagi, et al., Science **315**, 1380 (2007).
- [6] K. McElroy, R. W. Simmonds, J. E. Hoffman, D. H. Lee, J. Orenstein, H. Eisaki, S. Uchida, and J. C. Davis, Nature **422**, 592 (2003).
- [7] Y. Kohsaka, C. Taylor, P. Wahl, A. Schmidt, J. Lee, K. Fujita, J. W. Alldredge, K. McElroy, J. Lee, H. Eisaki, et al., Nature **454**, 1072 (2008).
- [8] N. Doiron-Leyraud, C. Proust, D. LeBoeuf, J. Levallois, J.-B. Bonnemaison, R. Liang, D. A. Bonn, W. N. Hardy, and L. Taillefer, Nature **447**, 565 (2007).
- [9] S. E. Sebastian, N. Harrison, E. Palm, T. P. Murphy, C. H. Mielke, R. Liang, D. A. Bonn, W. N. Hardy, and G. G. Lonzarich, Nature **454**, 200 (2008).
- [10] E.-A. Kim, M. J. Lawler, P. Oretto, S. Sachdev, E. Fradkin, and S. A. Kivelson, Phys. Rev. B **77**, 184514 (2008).
- [11] M. Chiao, R. W. Hill, C. Lupien, L. Taillefer, P. Lambert, R. Gagnon, and P. Fournier, Phys. Rev. B **62**, 3554 (2000).
- [12] M. F. Crommie, C. P. Lutz, and D. M. Eigler, Nature **363**, 524 (1993).
- [13] Q.-H. Wang and D.-H. Lee, Phys. Rev. B **67**, 020511 (2003).
- [14] T. Pereg-Barnea and M. Franz, Phys. Rev. B **68**, 180506 (2003).
- [15] A. V. Balatsky, I. Vekhter, and J.-X. Zhu, Rev. Mod. Phys. **78**, 373 (2006).
- [16] M. Vojta, Y. Zhang, and S. Sachdev, Phys. Rev. Lett. **85**, 4940 (2000).
- [17] V. Hinkov, D. Haug, B. Fauque, P. Bourges, Y. Sidis, A. Ivanov, C. Bernhard, C. T. Lin, and B. Keimer, Science **319**, 597 (2008).
- [18] K. Tanaka, W. S. Lee, D. H. Lu, A. Fujimori, T. Fujii, Risdiana, I. Terasaki, D. J. Scalapino, T. P. Devereaux, Z. Hussain, et al., Science **314**, 1910 (2006).
- [19] M. Le Tacon, A. Sacuto, A. Georges, G. Kotliar, Y. Gallais, D. Colson, and A. Forget, Nat Phys **2**, 537 (2006).
- [20] J. W. Alldredge, J. Lee, K. McElroy, M. Wang, K. Fujita, Y. Kohsaka, C. Taylor, H. Eisaki, S. Uchida, P. J. Hirschfeld, et al., Nature Physics **4**, 319 (2008).
- [21] K. McElroy, G.-H. Gweon, S. Y. Zhou, J. Graf, S. Uchida, H. Eisaki, H. Takagi, T. Sasagawa, D.-H. Lee, and A. Lanzara, Phys. Rev. Lett. **96**, 067005 (2006).
- [22] J. R. Schrieffer, *Theory of Superconductivity* (Westview Press, 1999).
- [23] M. R. Norman, M. Randeria, H. Ding, and J. C. Campuzano, Phys. Rev. B **52**, 615 (1995).
- [24] Y. Huh and S. Sachdev, Phys. Rev. B **78**, 064512 (2008).
- [25] T. Hanaguri et al., unpublished.

[1] V. Madhavan, K. Lang, E. Hudson, S. Pan, H. Eisaki, S. Uchida, and J. Davis, APS Meeting Abstracts pp.